Quasiballistic Magnetization Reversal

H. W. Schumacher,[1,*] C. Chappert,[1] R. C. Sousa,[2] P. P. Freitas,[2] and J. Miltat[3]

[1]*Institut d'Electronique Fondamentale, UMR 8622 CNRS, Université Paris Sud, Bâtiment 220, 91405 Orsay, France*
[2]*Instituto de Engenharia de Sistemas e Computadores, Rua Alves Redol 9, P-1000 Lisboa, Portugal*
[3]*Laboratoire de Physique des Solides, UMR 8502, CNRS, Université Paris Sud, Bâtiment 510, 91405 Orsay, France*

(Received 23 July 2002; published 8 January 2003)

We demonstrate a quasiballistic switching of the magnetization in a microscopic magnetoresistive memory cell. By means of time resolved magnetotransport, we follow the large angle precession of the free layer magnetization of a spin valve cell upon application of transverse magnetic field pulses. Stopping the field pulse after a 180° precession rotation leads to magnetization reversal with reversal times as short as 165 ps. This switching mode represents the fundamental ultrafast limit of field induced magnetization reversal.

DOI: 10.1103/PhysRevLett.90.017204 PACS numbers: 75.60.Jk, 85.70.Kh

The fundamental ultrafast limit of field induced magnetization reversal in ferromagnets is directly related to the precession frequency of the magnetization [1] upon application of a magnetic field pulse. When applying a field oriented mainly antiparallel to the initial magnetization $\boldsymbol{M}$, $\boldsymbol{M}$ has to undergo multiple precessional oscillations about the local effective field to reach full alignment with the reversed equilibrium direction [2–4]. The resulting reversal times are thus considerably longer than one precession period and are generally of the order of nanoseconds. A novel approach towards ultrafast magnetization reversal is the so-called precessional switching of magnetization [5–9]. Here, application of fast rising field pulses perpendicular to the initial direction of $\boldsymbol{M}$ initiates a large angle precession [10–12] that is used to reverse the magnetization. The ultimate switching speed could then be reached by stopping the field pulse exactly after a 180° precessional rotation [7,8]. This way, magnetization reversal in microscopic magnetic memory cells by field pulses as short as 140 ps has recently been demonstrated [13,14]. However, due to the lack of time resolution in these experiments, the effective reversal times are yet unknown and could be limited to several nanoseconds by the decay time of residual magnetic precession (''ringing'') upon field pulse termination [10–12]. According to theoretical predictions [8], however, an exact control of the pulse parameters should allow one to switch the magnetization on so-called ballistic trajectories characterized by the absence of ringing and thus to reach the fundamental limit of reversal speed.

In this Letter, we experimentally explore the fundamental limit of ultrafast magnetization reversal times in a microscopic memory cell. By measuring the time resolved magnetoresistance response of a spin valve during application of transverse field pulses, we follow the pronounced precession of the cell's free layer magnetization. Stopping the field pulse exactly after a half precessional rotation induces a quasiballistic reversal characterized by switching times as short as 165 ps and, within measurement accuracy, by a complete suppression of long wavelength magnetic excitations after field pulse decay.

An optical micrograph of a microscopic magnetic cell used in our experiments is shown in Fig. 1(a). The stadium shaped spin valve (SV) of 5 μm×2.3 μm lateral dimensions consists of Ta 65 Å/NiFe 40 Å/MnIr 80 Å/CoFe 43 Å/Cu 24 Å/CoFe 20 Å/NiFe 30 Å/Ta 8 Å. The exchange bias field defining the direction of the pinned magnetic layer and the magnetic easy axis of the free layer are oriented along the long dimension of the cell. The electrical contacts (C1,C2) allow one to measure the cell's giant magnetoresistance and thus to derive the average angle between the magnetization of the free and of the pinned layer [15]. Because of the overlap between the contact pads and the SV, the measured magnetoresistance (MR) is dominated by the magnetization orientation in the 2.1 μm wide center region not covered by the two contacts. The field pulses H_{pulse} are generated by current pulse injection into a buried pulse line (PL). All electrical lines are integrated into high bandwidth coplanar waveguides. Flowing a dc current through the SV during pulse application allows one to measure the SV's

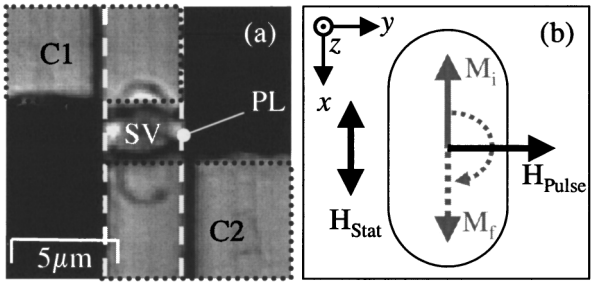

FIG. 1. Magnetic memory cell used in the experiments. (a) Optical micrograph. Spin valve cell (SV) with electrical contacts (C1, C2, surrounded by the dotted lines) and buried pulse line (PL, marked by the white dashed line). (b) Sketch of the magnetic field configuration H_{pulse} (along y) is applied perpendicular to the initial and final magnetization $\boldsymbol{M}_i$, $\boldsymbol{M}_f$.

ultrafast MR response using a 50 GHz sampling oscilloscope [16]. The current pulses are characterized after transmission through the device using a second oscilloscope channel. As sketched in Fig. 1(b), the field pulse H_{pulse} is applied along the in-plane magnetic hard axis, i.e., perpendicular to the initial and final direction of $\boldsymbol{M}$, whereas external static fields H_{stat} are applied along the easy axis by an external coil. The maximum pulsed fields obtained on this device are of the order of 280 Oe with pulse durations down to 170 ps and rise times as short as 45 ps (10% to 90% amplitude). For the sampling measurements, the pulses are applied with a repetition rate of 5 KHz. 2 μs after the fast pulse, a 140 ns, 80 Oe reset pulse generated by a second field line located on the back of the sample resets $\boldsymbol{M}$ to the initial state $\boldsymbol{M}_i$. By averaging over several hundred curves, low noise levels of the order of 50 μV are obtained [16] corresponding to an angular resolution down to 1.5°.

A static MR hysteresis loop of the SV is shown in Fig. 2(a). The coercivity H_C is 20 Oe and the loop is shifted to an offset field of $H_{\text{offset}} = 20$ Oe [17]. In the following, this offset field is always compensated by an external static field $H_{\text{stat}} = H_{\text{offset}}$. In the loop center, i.e., at offset compensation, the measured MR change due to the reversal of the free layer is of the order of 4%.

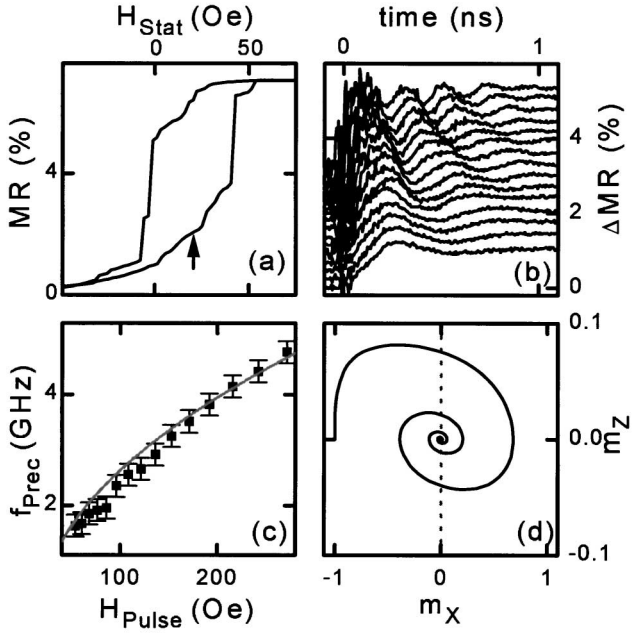

FIG. 2. (a) Easy axis MR loop of the spin valve. (b) Time resolved MR response of the SV to magnetic hard axis field steps from 52 Oe (bottom) to 272 Oe (top) in 1 dB increments. The MR data is offset for clarity. Precessional oscillations of the free layer about H_{pulse} are clearly observed. (c) Precession frequency f_{prec} vs applied field amplitude from Fourier transforms of the data in (b), and calculated values (gray line). (d) Calculated trajectory of the magnetization $\boldsymbol{M}$ in response o a field step of $H_{\text{pulse}} = 81$ Oe. m_X, m_Z are the normalized components of $\boldsymbol{M}$ along the easy axis, and out of plane, respectively [cf. Fig. 1(b)].

Figure 2(b) shows the time resolved MR response to the rise of hard axis field *steps* of amplitudes H_{pulse} between 53 and 272 Oe. The amplitude is varied in 1 dB increments. Pronounced oscillations of the MR are a clear indication of magnetic precession. From the exponential decay of the precession amplitude with time [8], we derive an effective damping parameter $\alpha = 0.03 \pm 0.005$. From Fourier transformation of the MR response, we obtain f_{prec}, the precession frequency under hard axis excitation, plotted in Fig. 2(c) vs field amplitude H_{pulse}. Kittel's formula for ferromagnetic resonance [18] captures the basic physics of the observed magnetization motion: The cell free layer is modeled as an ellipsoid with demagnetizing factors $N_X/4\pi = 0.0005$ (easy axis), $N_Y/4\pi = 0.002\,17$ (in-plane hard axis), and $N_Z/4\pi = 0.997\,33$ (out of plane) as suitable for the free layer geometry. Furthermore, the saturation magnetization $4\pi M_S = 10\,800$ Oe is assumed. The calculated dependence of $f_{\text{prec}}(H_{\text{pulse}})$ given by the gray straight line is in good agreement with the measured frequencies. The MR signal is clearly dominated by the free layer precession and not by the dynamics of the pinned layer of the SV [19]. In the following interpretation of the time resolved data, we thus neglect the pinned layer dynamics and directly calculate m_X, the component of $\boldsymbol{M}$ along the easy axis from the measured MR signal [15,20].

To model the time dependence of the magnetization response to the ultrashort hard axis pulses, we solve the Landau-Lifshitz-Gilbert equation [1], $d\boldsymbol{M}/dt = -\gamma(\boldsymbol{M} \times \boldsymbol{H}) + (\alpha/M_S)(\boldsymbol{M} \times d\boldsymbol{M}/dt)$, in the single spin (or macrospin) approximation. Here, γ is the gyromagnetic ratio, $\boldsymbol{H}$ the effective field, and α, M_S, the damping parameter and the saturation magnetization, respectively. The free layer is again modeled using the demagnetizing factors, saturation magnetization, and damping parameter given above. Furthermore, the pulse parameters used in the simulations mimic the shape and amplitude of the experimental pulses.

The simulated magnetization response to an 81 Oe field step along the in-plane hard axis is displayed in Fig. 2(d), showing the projection of the trajectory of $\boldsymbol{M}$ on the x, y plane. m_X is the normalized component of $\boldsymbol{M}$ along the easy axis and m_Z the out-of-plane component. $\boldsymbol{M}$ responds to the field step by damped precession about H_{pulse} starting from its initial position $\boldsymbol{M}_i$ (aligned along $-m_X$) and ending up being aligned with the hard axis field. Because of the sample's shape anisotropy and the resulting strong demagnetizing fields, $\boldsymbol{M}$ remains mainly in-plane (notice the different scales for m_X and m_Z). In Figs. 3(a) and 3(d), two calculated magnetization responses to short *pulses* are presented in the same way. The pulse in 3(a) has an amplitude of $H_{\text{pulse}} = 81$ Oe and a duration of $T_{\text{pulse}} = 175$ ps. Its time evolution is displayed in Fig. 3(b) (black line). During pulse application,

$\boldsymbol{M}$ performs approximately a half precession turn about H_{pulse} [see 3(a)]. At pulse decay time, $\boldsymbol{M}$ is oriented near the reversed easy axis direction $\boldsymbol{M}_f = -\boldsymbol{M}_i$ and relaxes towards it. The hard axis pulse is thus expected to induce a precessional switching of the magnetization. The measured field pulse (gray) is displayed in Fig. 3(b), whereas the measured (gray) and calculated (black) magnetization responses are given in Fig. 3(c), where m_X is plotted as a function of time. The measured time evolution of m_X is well described by the simple simulation. The short pulse induces precessional switching of the magnetization with ultrashort measured reversal time ($-0.9m_X$ to $+0.9m_X$) $T_{\text{switch}} = 165$ ps. Furthermore, no significant precession after pulse decay is present in m_X, neither in the measured data nor in the simulation and long wavelength magnetic excitations after pulse decay (ringing) are suppressed. The pulse very nearly matches the half precessional turn $T_{\text{pulse}} \approx \frac{1}{2} T_{\text{prec}}$ and, thus, the magnetization switches quasiballistically [8], i.e., with a close to optimum trajectory towards the reversed direction. This quasiballistic switching represents the fundamental ultrafast limit of field induced magnetization reversal for the given field amplitude.

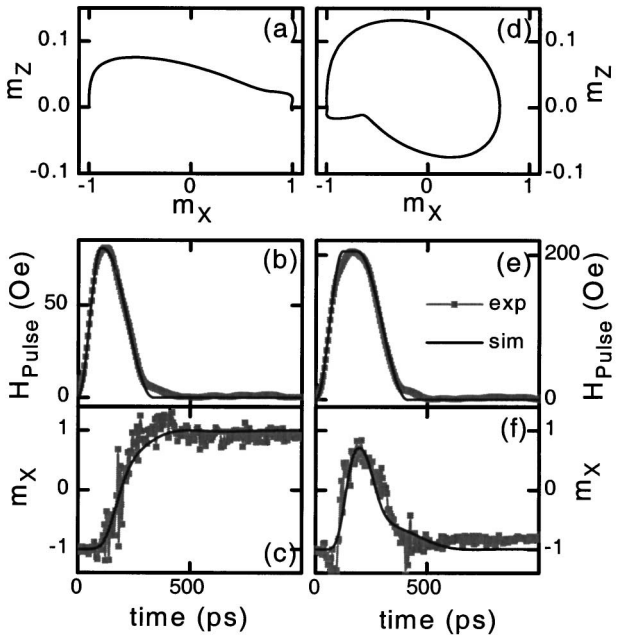

FIG. 3. Precessional switching of a SV cell. Calculated trajectories of precessional switching (a) and nonswitching (d) in the m_X-m_Z plane. For switching, the field pulse is stopped after a 180° precessional turn (a) ($H_{\text{pulse}} = 81$ Oe, $T_{\text{pulse}} = 175$ ps). Higher fields and longer pulse durations ($H_{\text{pulse}} = 205$ Oe, $T_{\text{pulse}} = 240$ ps) induce a full 360° rotation (d) (no switch). Field (b) and magnetization component m_X (c) vs time for $H_{\text{pulse}} = 81$ Oe, $T_{\text{pulse}} = 175$ ps. Gray dots: experiment; black lines: simulation. m_X switches within $T_{\text{switch}} = 165$ ps. No residual precession is found indicating quasiballistic reversal. Field (e) and m_X (f) vs time for $H_{\text{pulse}} = 205$ Oe, $T_{\text{pulse}} = 240$ ps.

The trajectory in Fig. 3(d) is the calculated response to a 205 Oe, 240 ps pulse. Because of the higher field and longer pulse duration time, $\boldsymbol{M}$ now performs a full 360° rotation about H_{pulse} before the pulse decays. Upon pulse termination, $\boldsymbol{M}$ is in this case oriented near the initial easy direction $\boldsymbol{M}_i$ and relaxes towards the latter. Therefore, in spite of strong precession during pulse application, no effective magnetization reversal takes place. The corresponding pulses and magnetization responses are found in Figs. 3(e) and 3(f), respectively. Now, during pulse application, m_X oscillates from the initial direction to the reversed orientation and back. The pulse matches here a full precessional rotation $T_{\text{pulse}} \approx T_{\text{prec}}$. Again, only little ringing is found following pulse termination.

For weak damping and sufficiently high field strengths [7,14], higher ratios of $T_{\text{pulse}}/T_{\text{prec}}$ can reveal consecutive regions of precessional higher order switching and nonswitching. Switching then occurs whenever $T_{\text{pulse}} \approx (n + \frac{1}{2})T_{\text{prec}}$ with $n = 0, 1, 2, \ldots$ being the order of the switching event. In contradistinction, no effective cell reversal will occur whenever $T_{\text{pulse}} \approx nT_{\text{prec}}$. This effect can be clarified using the macrospin trajectory in Fig. 2(d). Stopping the pulse at a point of the precession trajectory with a positive value of m_X (i.e., on the right-hand side of the dashed vertical line $m_X = 0$) will lead to relaxation into the reversed magnetization state (switch), whereas pulse termination at $m_X < 0$ will result in relaxation back to the initial state (no switch).

This oscillatory nature of precessional switching by hard axis pulses is well observed in Fig. 4. In 4(a), the measured response of m_X to a 305 ps, 272 Oe pulse is plotted as a function of time. In 4(b), the response of m_X to a series of pulses with $H_{\text{pulse}} = 272$ Oe [21] and $T_{\text{pulse}} = 200, \ldots, 900$ ps (10 ps increments) is plotted as a gray scale map, as a function of time and pulse duration. The curve in 4(a) is a section through the data in 4(b) along the horizontal dashed line. As seen in 4(a), the 305 ps pulse induces a first order ($n = 1$) precessional switch ($T_{\text{pulse}} \approx 1.5T_{\text{prec}}$). $\boldsymbol{M}$ rotates one and a half times about H_{pulse} during pulse application. However, the pulse parameters are not well tailored to 1.5 precessional rotations. As a consequence, $\boldsymbol{M}$ is not fully aligned with the reversed easy direction upon pulse termination resulting in a residual precession [see arrows (1)]. For the given pulse, full alignment of $\boldsymbol{M}$ with the final easy axis direction takes more than 1 ns. The precession limited effective reversal time is thus considerably longer than the switching pulse duration of only 305 ps. This emphasizes the importance of a precise control of the pulse parameters to achieve ultrafast quasiballistic switching.

The multiple oscillations of $\boldsymbol{M}$ about H_{pulse} for longer pulses can also be seen in Fig. 4(b). The oscillation maxima of m_X (light regions running vertically) are marked by the black dots and numbers 0–3 on the upper

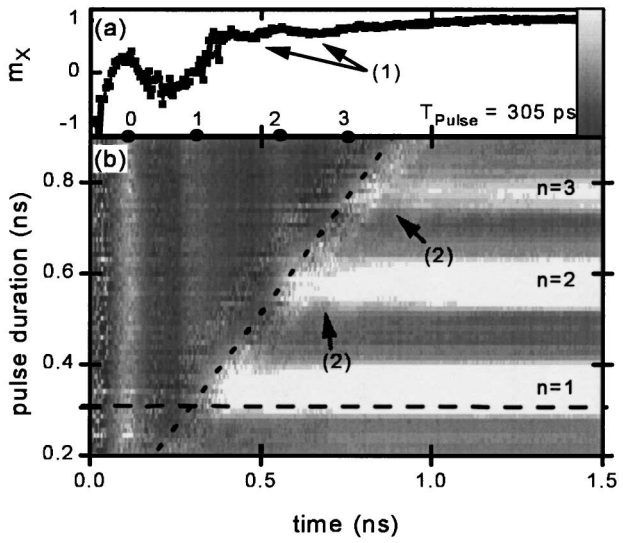

FIG. 4. Higher order precessional switching: (a) First order switch. Measured m_X vs time for $H_{\text{pulse}} = 272$ Oe, $T_{\text{pulse}} = 305$ ps. After pulse decay, residual precession occurs [arrows (1)]. (b) Gray scale encoded map of m_X as a function of time and pulse duration T_{pulse}. White: $m_X = 1$; dark gray: $m_X = -1$. $H_{\text{pulse}} = 272$ Oe [21]. Pulse field decays to zero along the inclined dotted line. Higher order switching (white horizontal regions, switching order n is indicated) occurs in phase with the precession at pulse cutoff. Zero order switching ($n = 0$) is not accessible for the given pulse amplitude.

border of the gray scale plot. The pulse decay is indicated in the data by the inclined dotted line. Pulse decay at a maximum of m_X (i.e., with $\boldsymbol{M}$ oriented near the reversed easy direction) inevitably leads to relaxation to the reversed easy axis direction, i.e., to high order precessional switching (white horizontal regions after pulse termination with switching order n). On the contrary, pulse decay at a minimum of m_X (i.e., with M oriented near the initial easy direction) always leads to relaxation towards the initial direction of $\boldsymbol{M}$ (gray horizontal regions) and no effective switching is monitored. Again, near the transition from switching to nonswitching, the alignment of $\boldsymbol{M}$ and the final easy axis direction is poor and a pronounced ringing of the magnetization upon pulse decay occurs [see, e.g., arrows (2)].

In conclusion, we have experimentally reached the fundamental ultrafast limit of field induced magnetization reversal of a microscopic magnetic memory cell. Quasiballistic magnetization switching with ultrashort reversal times of only 165 ps was demonstrated. The moderate field strength of 81 Oe and the low switch pulse energy of only 27 pJ for the present device demonstrates a high efficiency when compared to standard magnetization reversal schemes [2,3]. Such ballistic switching could, e.g., open the door to the ultrafast and yet low power magnetic random access memories [22,23] with clock rates well above the GHz.

We acknowledge financial support from EU Contracts No. HPMFCT02000-00540 and No. ERBFMRX-CT97-0147, and by a NEDO contract "Nanopatterned Magnets."

Note added.—After submission of this paper, similar results obtained in a magneto-optical experiment were published [24].

*Author to whom correspondence should be addressed. Electronic address: schumach@ief.u-psud.fr

[1] L. Landau and E. Lifshitz, Phys. Z. Sowjetunion **8**, 153 (1953); T. L. Gilbert, Phys. Rev. **100**, 1243 (1955).
[2] R. H. Koch *et al.*, Phys. Rev. Lett. **81**, 4512 (1998).
[3] B. C. Choi *et al.*, Phys. Rev. Lett. **86**, 728 (2001).
[4] W. K. Hiebert, G. E. Ballentine, and M. R. Freeman, Phys. Rev. B **65**, 140404(R) (2002).
[5] C. H. Back *et al.*, Phys. Rev. Lett. **81**, 3251 (1998).
[6] C. H. Back *et al.*, Science **285**, 864 (1999).
[7] M. Bauer *et al.*, Phys. Rev. B **61**, 3410 (2000).
[8] J. Miltat, G. Alburquerque, and A. Thiaville, in *Spin Dynamics in Confined Mangetic Structures*, edited by B. Hillebrands and K. Ounadjela (Springer-Verlag, Berlin, 2001).
[9] Y. Acreman *et al.*, Appl. Phys. Lett. **79**, 2228 (2001).
[10] W. K. Hiebert, A. Stankiewicz, and M. R. Freeman, Phys. Rev. Lett. **79**, 1134 (1997).
[11] Y. Acreman *et al.*, Science **290**, 492 (2000).
[12] T. M. Crawford *et al.*, Appl. Phys. Lett. **74**, 3386 (1999).
[13] S. Kaka and S. E. Russek, Appl. Phys. Lett. **80**, 2958 (2002).
[14] H.W. Schumacher *et al.*, Phys. Rev. Lett. **90**, 017201 (2003).
[15] B. Dieny *et al.*, Phys. Rev. B **43**, 1297 (1991).
[16] H.W. Schumacher *et al.*, Appl. Phys. Lett. **80**, 3781 (2002).
[17] D. Wang *et al.*, IEEE Trans. Magn. **36**, 2802 (2000).
[18] C. Kittel, *Introduction to Solid State Physics* (Wiley, New York, 1976), 5th ed.
[19] Simulations of the pinned layer dynamics including the exchange bias also show that pinned layer motion plays a minor role on the MR signal.
[20] m_X is proportional to the measured MR change due to the cosine angle dependence of the giant magnetoresistance.
[21] Nominally, $H_{\text{pulse}} = 272$ Oe. However, a linear decay of H_{pulse} with T_{pulse} down to 65% is found for $T_{\text{pulse}} <$ 300 ps.
[22] S. S. P. Parkin *et al.*, J. Appl. Phys. **85**, 5828 (1999).
[23] S. Tehrani *et al.*, IEEE Trans. Magn. **36**, 2752 (2000).
[24] Th. Gerrits *et al.*, Nature (London) **418**, 509 (2002); see also B. Hillebrands and J. Fassbender, Nature (London) **418**, 493 (2002).